

Supplementary Material

for

Oxidation of microcystin-LR via activation of peroxymonosulfate using ascorbic acid: Kinetic modeling and toxicity assessment

Shiqing Zhou,^{†,‡} Yanghai Yu,[†] Weiqiu Zhang,[‡] Xiaoyang Meng,[‡] Jinming Luo,[‡] Lin Deng,^{†,‡} Zhou

Shi[†] and John Crittenden ^{*,‡}

[†] Department of Water Engineering and Science, College of Civil Engineering, Hunan University,

Changsha, Hunan, 410082, China

[‡] Brook Byer Institute for Sustainable Systems and School of Civil and Environmental

Engineering, Georgia Institute of Technology, Atlanta, Georgia 30332, United States

Corresponding Author

John Crittenden

*E-mail: john.crittenden@ce.gatech.edu. Tel.: +1 404 894 5676; fax: +1 404 894 7896

Submitted to

Environmental Science & Technology

Number of pages (including this page): 23

Number of Text: 7

Number of Tables: 2

Number of Figures: 8

List of Supporting Information

Text S1. Chemicals.

Text S2. ESR Procedure for detection of sulfate and hydroxyl radicals.

Text S3. ESR Procedure for detection of ascorbyl radicals.

Text S4. Toxicity assessment of MCLR and its oxidation products.

Text S5. Modeling approach and rate constants determination.

Text S6. Kinetic equations.

Text S7. Energy costs for H₂A and PMS production.

Table S1. The objective function (OF) values for the kinetic model of MCLR degradation in the H₂A/PMS process.

Table S2. Oxidation products of MCLR identified by LC/MS/MS.

Figure S1. The calibration curve by plotting standards absorbance at 405 nm and concentration of MCLR (0.25-2.5 ug/L).

Figure S2. Proposed activated mechanism of PMS by ascorbic acid.

Figure S3. Model-predicted peroxymonosulfate radical (SO₅^{•-}) concentrations during the H₂A/PMS process.

Figure S4. Intensity profiles of hydroxyl radical, sulfate radical and ascorbyl radical during the H₂A/PMS process.

Figure S5. Fractions of H₂A, HA⁻ and A²⁻ species under different pH values.

Figure S6. Model-predicted sulfate radical and hydroxyl radical distributions under different NOM concentrations during the H₂A/PMS process.

Figure S7. EE/O_{total} (in kWh L⁻¹) of H₂A/PMS process vary with H₂A (a) and PMS (b) doses.

Figure S8. Proposed pathways of MC-LR degradation in the H₂A/PMS process.

Text S1 Chemicals

MCLR (>95%) centrifuged from *Microcystis aeruginosa* was purchased from Alexis Biochemicals (Switzerland). HPLC-grade acetonitrile, methanol and formic acid were obtained from Sigma-Aldrich (USA). Peroxymonosulfate (Oxone®, $\text{KHSO}_5 \cdot 0.5 \text{KHSO}_4 \cdot 0.5 \text{K}_2\text{SO}_4$, $\text{KHSO}_5 \geq 47\%$) was provided by Aladdin Co., Ltd. (Shanghai, China). 5,5-dimethyl-1-pyrrolidine N-oxide (DMPO) was obtained from Sigma-Aldrich (USA). Ascorbic acid, sodium hydroxide, sodium thiosulfate, sodium bicarbonate, potassium iodide and sulfuric acid were supplied by Sinopharm Chemical Reagent Co. (China). Suwannee River natural organic matter (NOM) was obtained from International Humic Substances Society (USA).

Text S2 ESR Procedure for detection of sulfate and hydroxyl radicals

The chemical of 5,5-dimethyl-1-pyrrolidine-N-oxide (DMPO) was used as a spin-trapping agent in the ESR experiment. The chemical solutions of DMPO, H₂A, and PMS were mixed for 15 seconds and immediately transferred into a 200 μ L capillary tube, which was then inserted into the cavity of the ESR spectrometer (Bruker A300, Germany). The total scanning time of the experiment was 30 minutes. The experiment was performed on the ESR spectrometer under the following conditions: a center field of 3361 Gs, a sweep width of 100 Gs, a microwave frequency of 9.420 GHz, a microwave power of 8.07 mW, a receiver gain of 4.48×10^4 , a modulation frequency of 100 KHz, a modulation amplitude of 1.0 Gs, and a sweep time of 30.72 seconds.

Text S3 ESR Procedure for detection of ascorbyl radicals

The ESR experiment for detection of ascorbyl radicals was conducted without any spin-trapping agent. The chemical solutions of H₂A and PMS were mixed for 15 seconds and immediately transferred into a 200 μ L capillary tube, which was then inserted into the cavity of the ESR spectrometer (Bruker A300, Germany). The total scanning time of the experiment was 30 minutes. The experiment was performed on the ESR spectrometer under the following conditions: a center field of 3513Gs, a sweep width of 100 Gs, a microwave frequency of 9.846 GHz, a microwave power of 8.08mW, a receiver gain of 4.48×10^4 , a modulation frequency of 100 KHz, a modulation amplitude of 1.0 Gs, and a sweep time of 30.72 seconds.

Text S4 Toxicity assessment of MCLR and its oxidation products

The hepatotoxicities of MCLR and its oxidation products were assessed by the PP2A activity assay using a MicroCystest kit (ZEU Immunotec, Spain). Typically, a calibration curve by plotting standards absorbance at 405 nm and concentration of MCLR (0.25-2.5 ug/L) is available in [Figure S1 \(SI\)](#). Samples were appropriately not within the range of the standard curve, and thus a dilution was made before PP2A analysis.

Text S5 Modeling approach and rate constants determination

The associated rate constants are generally drawn from the literature when we could find reported values. For the literature reported rate constants, most of them had a wide range. Consequently, the rate constants involving H_2A , HA^- and A^{2-} were obtained by fitting experimental data.

For model fits, the genetic algorithm (GA) was used to minimize the objective function (OF) and determine the rate constants.

$$OF = \sqrt{\frac{1}{n-1} \sum [(C_{exp} - C_{cal})/C_{exp}]^2} \quad (S1)$$

where n is the number of data points, C_{exp} and C_{cal} are the experimental and calculated concentrations of MCLR, respectively.

The kinetic equations used in the model were derived from the mass balance for a species, A, in a completely mixed batch reactor (CMBR), yielding the following ordinary differential equations (ODEs):¹

$$\frac{dC_a}{dt} = r_a, \quad C_a|_{t=0} = C_{a0} \quad (S2)$$

Where, C_{a0} is the initial concentration of species A at time 0, C_a is the concentration of A at time t , and r_a is the overall kinetic rate expression of species A in the reaction system. The backward differentiation formula (BDF) method [i.e., Gear's method]² was used to solve all differential equations and obtain the concentration profiles of all species in MATLAB.³

Text S6 Kinetic equations

Based on the reactions in Table 1, the overall kinetic rate expressions can be written for inclusion in equation S2.

$$\begin{aligned}
 \frac{d[SO_4^- \bullet]}{dt} = & k_1[H_2A][HSO_5^-] + k_2[HA^-][HSO_5^-] - k_3[H_2O][SO_4^- \bullet] \\
 & - k_4[H_2O][SO_4^- \bullet] - k_5[[H_2A]][SO_4^- \bullet] - k_6[HA^-][SO_4^- \bullet] \\
 & - k_9[HSO_5^-][SO_4^- \bullet] + k_{10}[HSO_5^-][HO \bullet] - k_{12}[A^- \bullet][SO_4^- \bullet] \\
 & - 2k_{14}[SO_4^- \bullet][SO_4^- \bullet] - k_{15}[SO_5^- \bullet][SO_4^- \bullet] - k_{21}[H_2O_2][SO_4^- \bullet] \\
 & - k_{22}[HO_2 \bullet][SO_4^- \bullet] - k_{23}[HO \bullet][SO_4^- \bullet] - k_{27}[MCLR][SO_4^- \bullet]
 \end{aligned} \tag{S3}$$

$$\begin{aligned}
 \frac{d[OH \bullet]}{dt} = & k_3[H_2O][SO_4^- \bullet] + k_4[H_2O][SO_4^- \bullet] - k_7[H_2A][HO \bullet] - k_8[HA^-][HO \bullet] \\
 & - k_{10}[HSO_5^-][HO \bullet] - k_{13}[A^- \bullet][HO \bullet] - 2k_{16}[HO \bullet][HO \bullet] \\
 & - k_{17}[H_2O_2][HO \bullet] - k_{18}[HO_2 \bullet][HO \bullet] - k_{26}[S_2O_8^{2-}][HO \bullet] \\
 & - k_{28}[MCLR][OH \bullet]
 \end{aligned} \tag{S4}$$

$$\begin{aligned}
 \frac{d[A^- \bullet]}{dt} = & k_1[H_2A][HSO_5^-] + k_2[HA^-][HSO_5^-] + k_5[[H_2A]][SO_4^- \bullet] \\
 & + k_6[HA^-][SO_4^- \bullet] + k_7[H_2A][HO \bullet] + k_8[HA^-][HO \bullet] \\
 & - 2k_{11}[A^- \bullet][A^- \bullet] - k_{12}[A^- \bullet][SO_4^- \bullet] - k_{13}[A^- \bullet][HO \bullet]
 \end{aligned} \tag{S5}$$

$$\begin{aligned}
 \frac{d[SO_5^- \bullet]}{dt} = & k_9[HSO_5^-][SO_4^- \bullet] - k_4[H_2O][SO_4^- \bullet] - k_{15}[SO_5^- \bullet][SO_4^- \bullet] \\
 & - 2k_{24}[SO_5^- \bullet][SO_5^- \bullet] - 2k_{25}[SO_5^- \bullet][SO_5^- \bullet]
 \end{aligned} \tag{S6}$$

$$\begin{aligned}\frac{d[HSO_5^-]}{dt} = & -k_1[H_2A][HSO_5^-] - k_2[HA^-][HSO_5^-] - k_9[HSO_5^-][SO_4^- \bullet] \\ & - k_{10}[HSO_5^-][HO \bullet]\end{aligned}\tag{S7}$$

$$\frac{d[H_2A]}{dt} = -k_1[H_2A][HSO_5^-] - k_5[[H_2A]][SO_4^- \bullet] - k_7[H_2A][HO \bullet]\tag{S8}$$

$$\frac{d[HA^-]}{dt} = -k_2[HA^-][HSO_5^-] - k_6[HA^-][SO_4^- \bullet] - k_8[HA^-][HO \bullet]\tag{S9}$$

$$\begin{aligned}\frac{d[S_2O_8^{2-}]}{dt} = & k_{14}[SO_4^- \bullet][SO_4^- \bullet] + k_{15}[SO_5^- \bullet][SO_4^- \bullet] + k_{24}[SO_5^- \bullet][SO_5^- \bullet] \\ & - k_{26}[S_2O_8^{2-}][HO \bullet]\end{aligned}\tag{S10}$$

$$\begin{aligned}\frac{d[H_2O_2]}{dt} = & k_{16}[HO \bullet][HO \bullet] - k_{17}[H_2O_2][HO \bullet] + 2k_{19}[HO_2 \bullet][HO_2 \bullet] \\ & - k_{20}[H_2O_2][HO_2 \bullet] - k_{21}[H_2O_2][SO_4^- \bullet]\end{aligned}\tag{S11}$$

$$\begin{aligned}\frac{d[HO_2 \bullet]}{dt} = & k_{17}[H_2O_2][HO \bullet] - k_{18}[HO_2 \bullet][HO \bullet] - k_{19}[HO_2 \bullet][HO_2 \bullet] \\ & - k_{20}[H_2O_2][HO_2 \bullet] + k_{21}[H_2O_2][SO_4^- \bullet] - k_{22}[HO_2 \bullet][SO_4^- \bullet]\end{aligned}\tag{S12}$$

$$\frac{d[MCLR]}{dt} = -k_{27}[MCLR][SO_4^- \bullet] - k_{28}[MCLR][HO \bullet]\tag{S13}$$

Text S7 Energy costs for H₂A and PMS production

The local costs of H₂A and PMS are estimated to be 2.5 \$ kg⁻¹ and 3.0 \$ kg⁻¹, respectively. And the local electricity cost in Georgia (USA) is 0.065 \$ kWh⁻¹. According to the method of Rosenfeldt et al.,⁴ the energy costs for H₂A and PMS production were calculated to be 17.44 and 20.93 kWh lb⁻¹, respectively.

H₂A cost=\$ 2.5 kg⁻¹

PMS cost=\$ 3.0 kg⁻¹

Local electricity cost = \$ 0.065 kWh⁻¹

Energy cost of H₂A=38.46 kWh kg⁻¹=17.44 kWh lb⁻¹

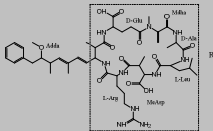
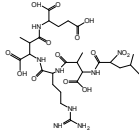
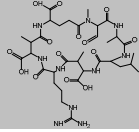
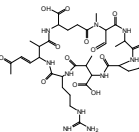
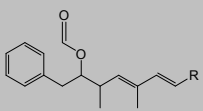
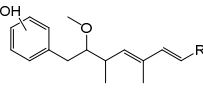
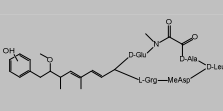
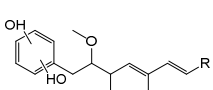
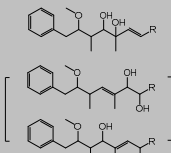
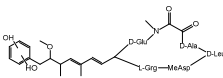
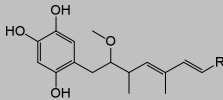
Energy cost of PMS=46.15 kWh kg⁻¹=20.93 kWh lb⁻¹

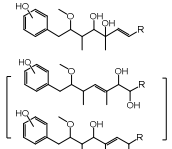
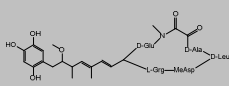
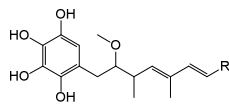
Table S1 The objective function (OF) values for the kinetic model of MCLR degradation in the H₂A/PMS process.

Kinetic model				Different solution pH values		In the presence of NOM	
[H ₂ A]	OF _{H₂A}	[PMS]	OF _{PMS}	pH	OF _{pH}	NOM	OF _{NOM}
1	0.09	1	0.05	4	0.11	0	0.11
2	0.11	2	0.10	5	0.10	1	0.11
5	0.26	5	0.11	6	0.10	3	0.08
10	0.06	10	0.17	-	-	5	0.06

The unit of H₂A and PMS was μM ; the unit of NOM was mg L^{-1} .

Table S2 Oxidation products of MCLR identified by LC/MS/MS

Product No.	Chemical formula [M+H] ⁺	Structure formula	m/z	RT (min)	References
MCLR	C ₄₉ H ₇₅ N ₁₀ O ₁₂		995.6000	10.177	-
1	C ₂₇ H ₄₅ N ₈ O ₁₄		705.5000	19.043	5
2	C ₃₄ H ₅₅ N ₁₀ O ₁₄		827.5000	43.296	5
3	C ₃₇ H ₅₉ N ₁₀ O ₁₃		851.0000	28.301	6, 7
4	C ₄₉ H ₇₃ N ₁₀ O ₁₃		1009.5000	30.660	8, 9
5	C ₄₉ H ₇₅ N ₁₀ O ₁₃		1011.5000	51.573	8-12
6	C ₄₈ H ₇₃ N ₁₀ O ₁₄		1013.5000	0.369,11.609	7
7	C ₄₉ H ₇₅ N ₁₀ O ₁₄		1027.5000	41.087,41.584,43.364	8-12
8	C ₄₉ H ₇₇ N ₁₀ O ₁₄		1029.5000	20.355	5
9	C ₄₈ H ₇₃ N ₁₀ O ₁₅		1029.5000	20.355	7
10	C ₄₉ H ₇₅ N ₁₀ O ₁₅		1042.5000	6.641,36.428	5

11	$C_{49}H_{78}N_{10}O_{15}$		1045.5000	3.520	5
12	$C_{48}H_{73}N_{10}O_{16}$		1045.5000	3.520	7
13	$C_{49}H_{75}N_{10}O_{16}$		1058.5000	54.612	No literature

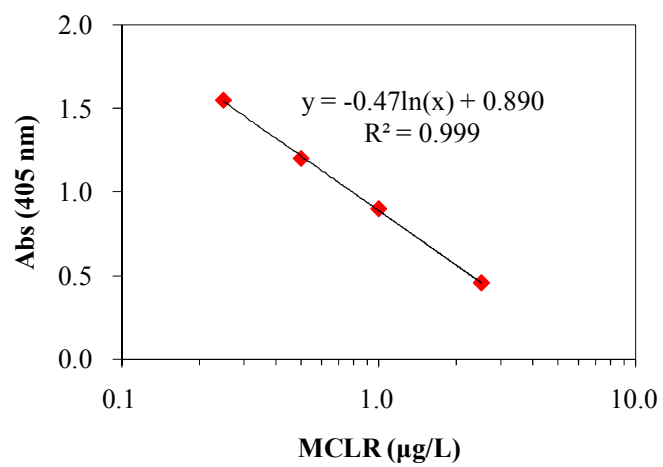


Figure S1 The calibration curve by plotting standards absorbance at 405 nm and concentration of MCLR (0.25-2.5 ug/L).

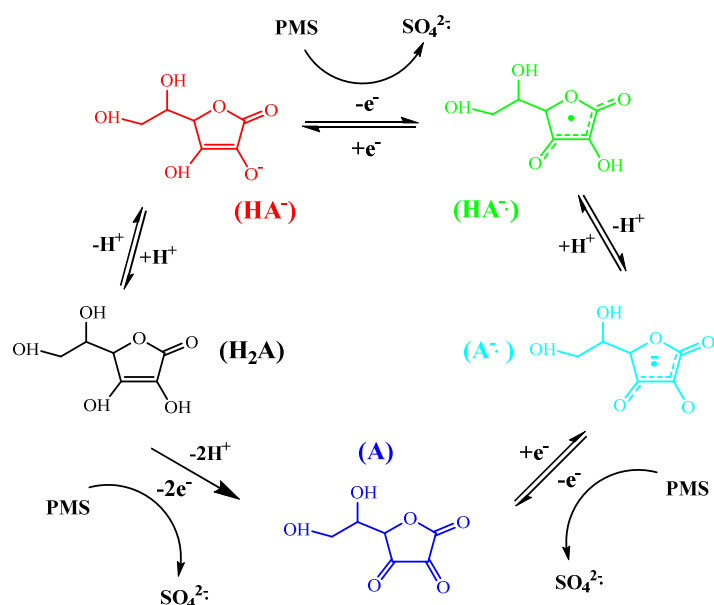


Figure S2 Proposed activated mechanism of PMS by ascorbic acid. Typically, ascorbic acid (H_2A) has two ionizable $-OH$ groups, and a dissociation constant in water of 7.94×10^{-5} ($pK_a=4.2$). At neutral pH, the ascorbate monoanion (HA^-) is the dominant species. HA^- can donate one electron to produce semidehydroascorbate radical, which is oxidized to form the ascorbyl radical ($A^{\bullet-}$). At the same time, PMS can receive the donated one electron and generate $SO_4^{\bullet-}$, and partial $SO_4^{\bullet-}$ can further react with OH^- or H_2O to produce HO^{\bullet} . Then, the ascorbyl radical can donate another electron to produce dehydroascorbic acid (A) and also activate PMS to generate $SO_4^{\bullet-}$. The dehydroascorbic acid is unstable and breaks down rapidly into diketo-L-gulonic acid, which ultimately produces oxalic and L-threonic acids¹³. Meanwhile, ascorbic acid (H_2A) can also directly donate two electrons to produce dehydroascorbic acid (A) and activate PMS to generate $SO_4^{\bullet-}$.

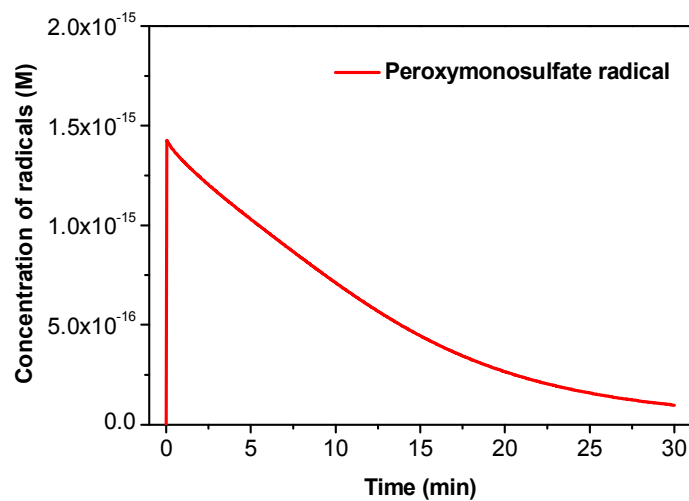


Figure S3 Model-predicted peroxymonosulfate radical (SO₅•-) concentrations during the H₂A/PMS process. Conditions: H₂A = 2.0 × 10⁻⁶ M, PMS = 5.0 × 10⁻⁶ M, and pH₀ = 4.0.

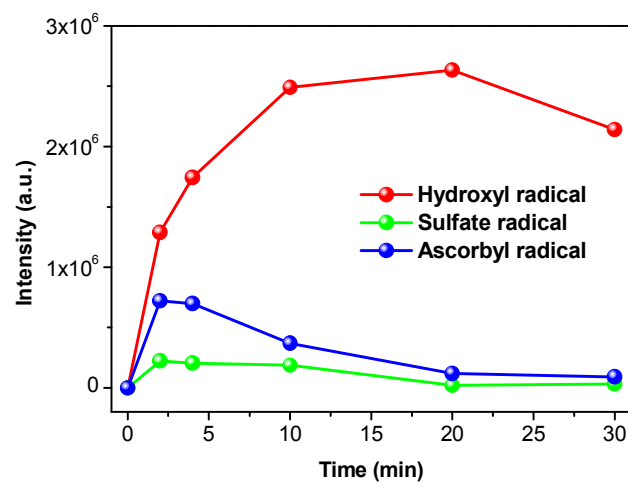


Figure S4 Intensity profiles of hydroxyl radical, sulfate radical and ascorbyl radical during the H₂A/PMS process.

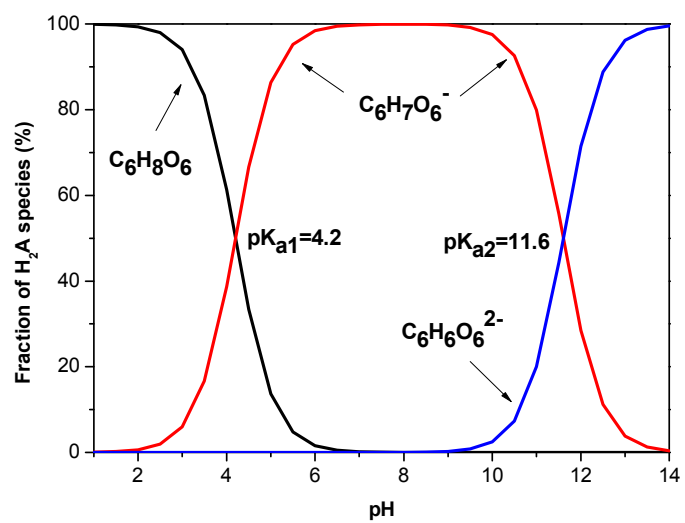


Figure S5 Fractions of H₂A, HA⁻ and A²⁻ species under different pH values.

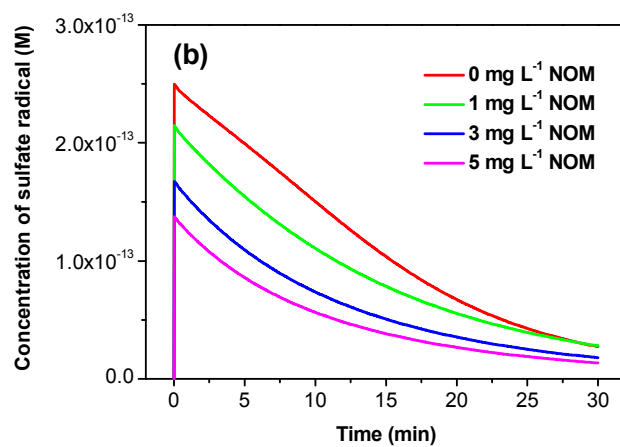
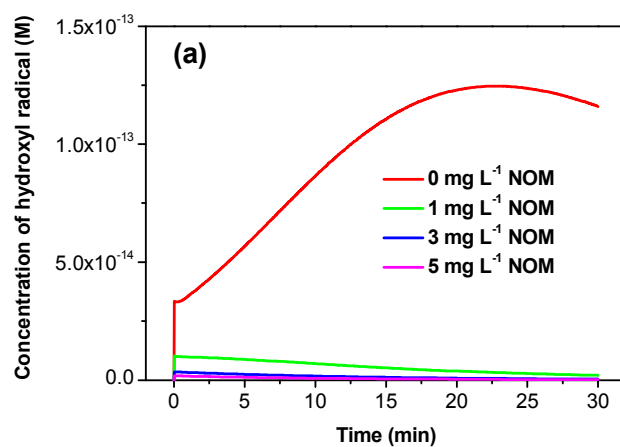


Figure S6 Model-predicted sulfate radical and hydroxyl radical distributions under different NOM concentrations during the H₂A/PMS process. Conditions: [MCLR]₀ = 2.0 × 10⁻⁷ M, H₂A = 2.0 × 10⁻⁶ M, PMS = 5.0 × 10⁻⁶ M, and pH₀ = 4.0.

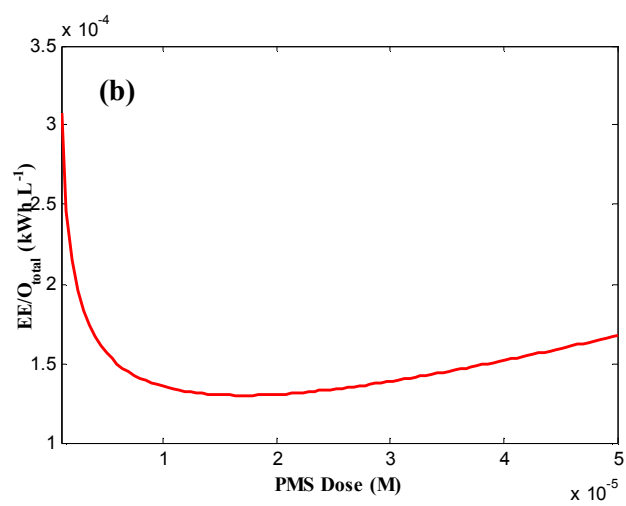
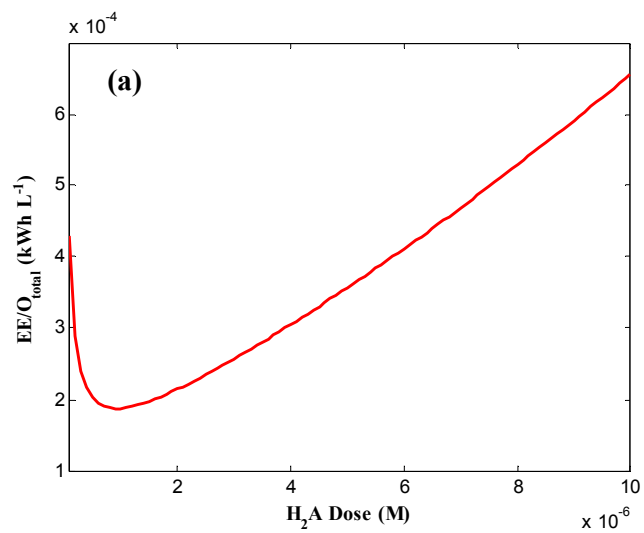


Figure S7 $\text{EE}/\text{O}_{\text{total}}$ (in kWh L^{-1}) of $\text{H}_2\text{A}/\text{PMS}$ process vary with H_2A (a) and PMS (b) doses. Conditions: $[\text{MCLR}]_0 = 2.0 \times 10^{-7}$ M, $\text{H}_2\text{A} = 1.0 \times 10^{-7}$ - 1.0×10^{-5} M, $\text{PMS} = 1.0 \times 10^{-6}$ - 5×10^{-5} M, and $\text{pH}_0 = 4.0$.

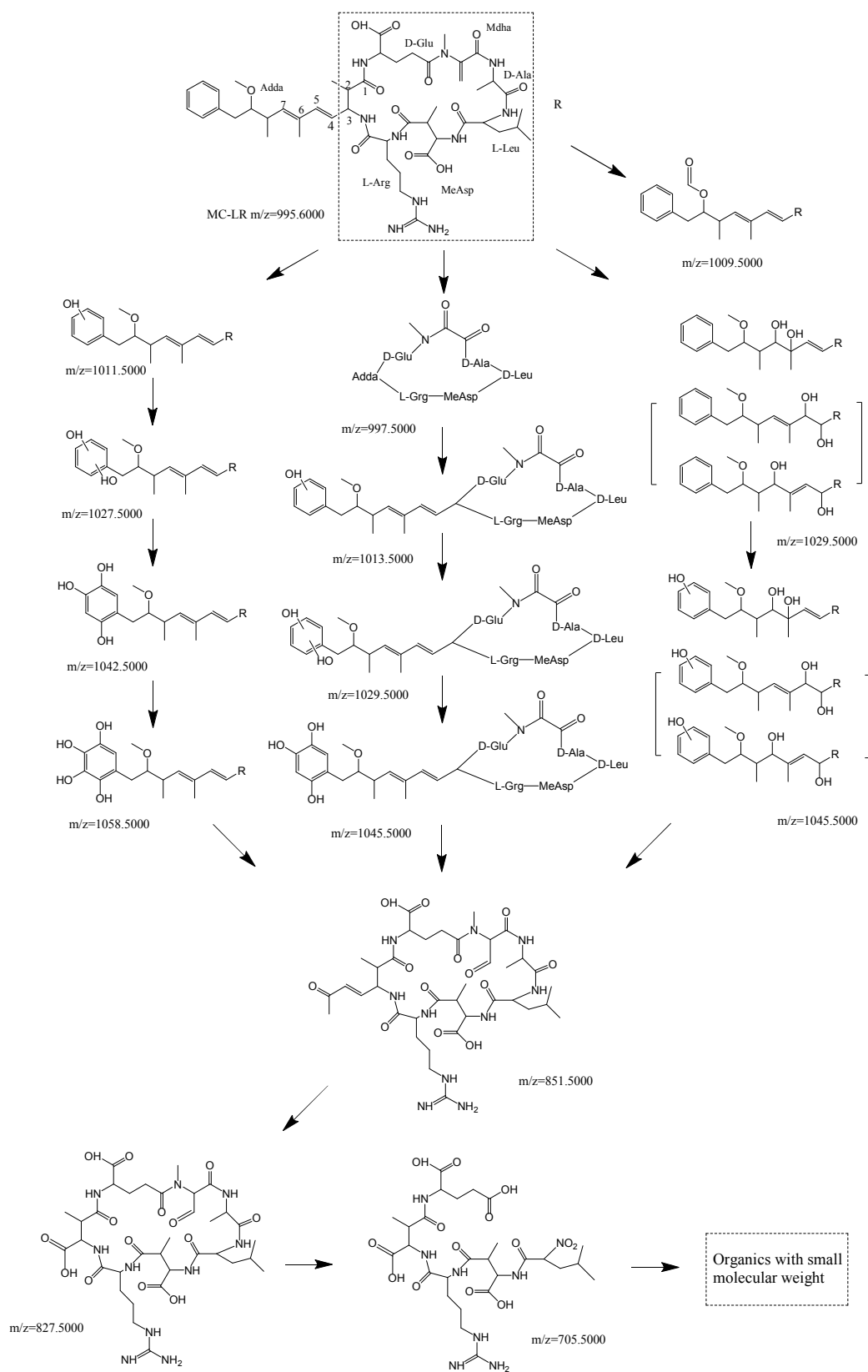


Figure S8 Proposed pathways of MC-LR degradation in the H_2A/PMS process.

Reference

- (1) Crittenden, J. C.; Hu, S.; Hand, D. W.; Green, S. A., A kinetic model for H₂O₂/UV process in a completely mixed batch reactor. *Water Res.* **1999**, *33* (10), 2315-2328.
- (2) Gear, C. W.; Petzold, L. R., ODE methods for the solution of differential/algebraic systems. *SIAM J. Numer. Anal.* **1984**, *21* (4), 716-728.
- (3) Qian, Y.; Guo, X.; Zhang, Y.; Peng, Y.; Sun, P.; Huang, C.-H.; Niu, J.; Zhou, X.; Crittenden, J. C., Perfluorooctanoic Acid Degradation Using UV–Persulfate Process: Modeling of the Degradation and Chlorate Formation. *Environ. Sci. Technol.* **2015**, *50* (2), 772-781.
- (4) Rosenfeldt, E. J.; Linden, K. G.; Canonica, S.; Von Gunten, U., Comparison of the efficiency of OH radical formation during ozonation and the advanced oxidation processes O₃/H₂O₂ and UV/H₂O₂. *Water Res.* **2006**, *40* (20), 3695-3704.
- (5) Zhou, S.; Bu, L.; Yu, Y.; Zou, X.; Zhang, Y., A comparative study of microcystin-LR degradation by electrogenerated oxidants at BDD and MMO anodes. *Chemosphere* **2016**, *165*, 381-387.
- (6) Fang, Y.; Zhang, Y.; Ma, W.; Johnson, D. M.; Huang, Y.-p., Degradation of microcystin-LR in water: hydrolysis of peptide bonds catalyzed by maghemite under visible light. *Appl. Catal. B: Environ.* **2014**, *160*, 597-605.
- (7) Kim, M. S.; Kim, H.-H.; Lee, K.-M.; Lee, H.-J.; Lee, C., Oxidation of microcystin-LR by ferrous-tetrapolyphosphate in the presence of oxygen and hydrogen peroxide. *Water Res.* **2017**, *114*, 277-285.
- (8) Antoniou, M. G.; Shoemaker, J. A.; Cruz, A. A. d. l.; Dionysiou, D. D., Unveiling new degradation intermediates/pathways from the photocatalytic degradation of microcystin-LR. *Environ. Sci. Technol.* **2008**, *42* (23), 8877-8883.

- (9) Yanfen, F.; Yingping, H.; Jing, Y.; Pan, W.; Genwei, C., Unique ability of BiOBr to decarboxylate D-Glu and D-MeAsp in the photocatalytic degradation of microcystin-LR in water. *Environ. Sci. Technol.* **2011**, *45* (4), 1593-1600.
- (10) Antoniou, M. G.; de la Cruz, A. A.; Dionysiou, D. D., Intermediates and reaction pathways from the degradation of microcystin-LR with sulfate radicals. *Environ. Sci. Technol.* **2010**, *44* (19), 7238-7244.
- (11) Jiang, W.; Chen, L.; Batchu, S. R.; Gardinali, P. R.; Jasa, L.; Marsalek, B.; Zboril, R.; Dionysiou, D. D.; O' Shea, K. E.; Sharma, V. K., Oxidation of microcystin-LR by ferrate (VI): kinetics, degradation pathways, and toxicity assessments. *Environ. Sci. Technol.* **2014**, *48* (20), 12164-12172.
- (12) He, X.; Armah, A.; Hiskia, A.; Kaloudis, T.; O'Shea, K.; Dionysiou, D. D., Destruction of microcystins (cyanotoxins) by UV-254 nm-based direct photolysis and advanced oxidation processes (AOPs): Influence of variable amino acids on the degradation kinetics and reaction mechanisms. *Water Res.* **2015**, *74*, 227-238.
- (13) Nappi, A. J.; Vass, E., Hydroxyl radical production by ascorbate and hydrogen peroxide. *Neurotox. Res.* **2000**, *2* (4), 343-355.